Topological phase transition in a generalized Kane-Mele-Hubbard model: A combined quantum Monte Carlo and Green's function study

Hsiang-Hsuan Hung, Lei Wang, Zheng-Cheng Gu, and Gregory A. Fiete

Topological phase transition in a generalized Kane-Mele-Hubbard model: A combined Quantum Monte Carlo and Green's function study

Hsiang-Hsuan Hung,[1] Lei Wang,[2] Zheng-Cheng Gu,[3, 4] and Gregory A. Fiete[1]

[1]*Department of Physics, The University of Texas at Austin, Austin, TX, 78712, USA*
[2]*Theoretische Physik, ETH Zurich, 8093 Zurich, Switzerland*
[3]*Institute for Quantum Information, California Institute of Technology, Pasadena, CA 91125, USA*
[4]*Department of Physics, California Institute of Technology, Pasadena, CA 91125, USA*
(Dated: March 12, 2013)

We study a generalized Kane-Mele-Hubbard model with third-neighbor hopping, an interacting two-dimensional model with a topological phase transition as a function of third-neighbor hopping, by means of the determinant projector Quantum Monte Carlo (QMC) method. This technique is essentially numerically exact on models without a fermion sign problem, such as the one we consider. We determine the interaction-dependence of the Z_2 topological insulator/trivial insulator phase boundary by calculating the Z_2 invariants directly from the single-particle Green's function. The interactions push the phase boundary to larger values of third-neighbor hopping, thus stabilizing the topological phase. The observation of boundary shifting entirely stems from quantum fluctuations. We also identify qualitative features of the single-particle Green's function which are computationally useful in numerical searches for topological phase transitions without the need to compute the full topological invariant.

Introduction.-Recently, interest in a new state of matter, topological insulators, has exploded.[1–6] Z_2 topological insulators (TI) do not require interactions for their existence. However, intermediate strength electron-electron interactions have been shown to drive novel phases in slave-particle studies when the non-interacting limit is a TI.[7–12] Interaction effects have also appeared in experimental studies on the weakly correlated Bi-based TI.[13,14] Moreover, a recently discovered Kondo topological insulator[15] seems a promising venue to explore the strongly interacting limit. An essential challenge in many-body studies of TI systems is the direct characterization of the interacting topological phases and phase transitions. This has largely been accomplished with either mean-field-like approaches or indirect evidence (such as the spontaneous appearance of an order parameter, or the closing of the single-particle excitation gap). Thus, it is important to understand the role of interactions in topological phases beyond the standard independent-particle and mean-field framework, ideally within an unbiased approach.

Various approaches, including the entanglement entropy/spectrum[16,17] or K-matrix theory[18] have also been proposed to characterize these topological phases. In the case of Z_2 TI, topological invariants can be identified in terms of the single-particle Green's function.[19–21] In certain cases, the frequency domain-winding-number[22] and a pole-expansion of the self-energy[23] could be useful in identifying interaction effects in a topological phase transition. The pole-structure of the Green's function in dynamical mean-field theory has been shown to be a powerful tool in the study of interaction effects in topological phases.[24] The approach, however, still faces the limitation of being applicable only to local self-energy approximations.

Interaction induced topological phase transitions have been studied in various models, including the Haldane-Hubbard model,[25,26] the Kane-Mele-Hubbard model[27–32] and the interacting Bernevig-Hughes-Zhang model.[33–35] Within these models, there is also a topological phase transition at the single-particle level even without interaction,[36] which can be induced by a staggered on-site energy,[37] Rashba spin-orbit coupling,[37,38] or a third-neighbor hopping, as we discuss in this Rapid Communication. To study this transition we use numerically exact determinant projector QMC to map out the interaction dependence of the topological phase transition as a function of third-neighbor hopping. We find that interactions tend to stabilize the topological phase, and we show the zero-frequency behavior of the Green's function as a function of third-neighbor hopping can be used to quantitatively determine the phase boundary.

Model.-We consider the generalized Kane-Mele-Hubbard model (KMH) on the honeycomb lattice (unit cell sites labeled A and B) with real-valued third-neighbor hopping t_{3N}: $H = H_0 + H_U$ with

$$H_0 = -t \sum_{\langle i,j \rangle} \sum_{\sigma} c_{i\sigma}^\dagger c_{j\sigma} + i\lambda_{SO} \sum_{\langle\langle i,j \rangle\rangle} \sum_{\sigma} \sigma c_{i\sigma}^\dagger \nu_{ij} c_{j\sigma}$$
$$- t_{3N} \sum_{\langle\langle\langle i,j \rangle\rangle\rangle} \sum_{\sigma} c_{i\sigma}^\dagger c_{j\sigma}, \tag{1}$$

and $H_U = \frac{U}{2} \sum_i (n_i - 1)^2$. Here $c_{i,\sigma}^\dagger$ creates an electron with spin-σ on site-i; the fermion number operator is $n_i = \sum_\sigma c_{i,\sigma}^\dagger c_{i,\sigma}$; σ runs over $\uparrow$ and $\downarrow$. The spin-orbit coupling strength is λ_{SO}, and $\nu_{ij} = +1$ for counter-clockwise hopping with $\nu_{ij} = -1$ otherwise.[37] The spin-orbit coupling term opens a bulk gap and drives the system to a Z_2 TI for $t_{3N} = 0$.[37]

The Brillouin zone (BZ) of the honeycomb lattice is
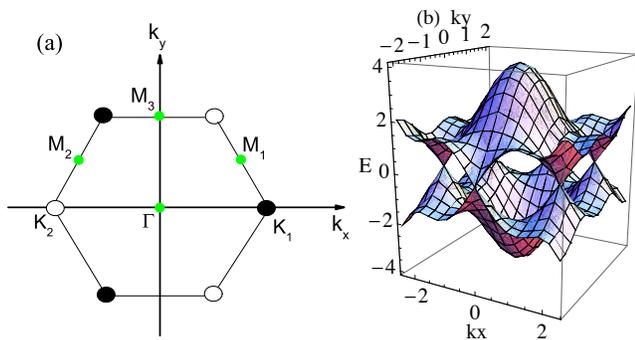
FIG. 1: (Color online) (a) The first Brillouin zone of the honeycomb lattice. For $t_{3N} = 0$, the Dirac points are located at $K_{1,2} = (\pm\frac{4\pi}{3\sqrt{3}a}, 0)$ labeled by open and solid circles, respectively. The time-reversal invariant momentum (TRIM) points labeled by the green dots are $\Gamma = (0,0)$, $M_{1,2} = (\pm\frac{\pi}{\sqrt{3}a}, \frac{\pi}{3a})$, and $M_3 = (0, \frac{2\pi}{3a})$. (b) The noninteracting band structure of the generalized KM model Eq.(1) at $t_{3N} = \frac{1}{3}t$ (here using $\lambda_{SO} = 0.3t$). Note that at the critical point separating the trivial insulator from the TI the Dirac cones shift to the TRIM points $M_{1,2,3}$, instead at $K_{1,2}$.

shown in Fig. 1 (a). For general t_{3N} but vanishing λ_{SO}, the model still exhibits a graphene-like band structure with gapless Dirac cones located at $K_{1,2} = (\pm\frac{4\pi}{3\sqrt{3}a}, 0)$, where a is the lattice constant. However, an arbitrary λ_{SO} will open a bulk gap and the generalized KM model turns into a Z_2 TI or a trivial insulator depending on values of t_{3N}. We find that for $U = 0$ the critical value of the third-neighbor coupling t_c is $t_{3N} = \frac{1}{3}t$. At t_c, the bulk gap closes and the gapless Dirac cones shift away from the K points and move to time-reversal invariant momenta (TRIM), $M_{1,2} = (\pm\frac{\pi}{\sqrt{3}a}, \frac{\pi}{3a})$ and $M_3 = (0, \frac{2\pi}{3a})$. The band structure at the topological critical point is depicted in Fig. 1 (b). As $t_{3N} < \frac{1}{3}t$, the system is a Z_2 TI, whereas as $t_{3N} > \frac{1}{3}t$ it is a trivial insulator. At the noninteracting level, the value of t_c is independent of λ_{SO}.

We next consider the Hubbard interaction H_U, given below Eq.(1). In the presence of the Hubbard interaction, the topological phase boundary, t_c, shifts; a mean-field approach is unable to accurately determine t_c for $U \neq 0$. In fact, we have verified that Hartree-Fock theory[39] predicts no shift at all for U sufficiently small to avoid the magnetic transition. For U larger than this critical value, U_c, the topological band insulator state breaks down to a topologically trivial magnetic state.[27–32] Since the generalized Kane-Mele Hubbard model we consider with the t_{3N} term still preserves the essential band features of the Kane-Mele model, one can expect that in the strong coupling limit $U > U_c$ our generalized model will also have a phase transition from the Z_2 TI to the magnetic state.

To study physics not captured within a mean-field theory, we choose a moderate Hubbard interaction U relative to the bandwidth (small enough to avoid inducing the magnetic phase in the thermodynamic limit). Our

main goal here is to demonstrate how the single-particle Green's functions computed within QMC in a fermion sign-free problem can be used to identify a correlated TI phase and topologically trivial insulating state. We leave a detailed analysis of the large U case for a future publication. At half-filling, *i.e.,* one fermion per site, the system has a particle-hole symmetry and the QMC simulations can perform accurate sampling without sign problems. Thus, one can accurately determine the phase boundary shifts at different U beyond the mean-field level. We find that as U increases, the critical value of t_{3N} shifts towards a larger value, thus effectively *stabilizing* the Z_2 TI phase.

Numerical Results.-In our QMC calculations we use an imaginary time step $\Delta\tau$ such that $\Delta\tau t = 0.05$ and an inverse temperature Θ such that $\Theta t = 40$. For the noninteracting case, for any finite λ_{SO} and at $t_{3N} < t_c$, the system is a Z_2 TI. We find that for $\lambda_{SO} = 0.1t$, the model transitions to a magnetic state at $U = 3t$. To increase the threshold value of U needed to induce the magnetism, we consider a larger $\lambda_{SO} = 0.4t$ or even $\lambda_{SO} = t$ for different U. For comparison, in Fig. 2 we plot the value of the Z_2 invariant as a function of t_{3N} for different values of U. Open and solid symbols denote the noninteracting and interacting cases, respectively. Unless otherwise stated, we consider system sizes $L \times L = 6 \times 6$ with periodic boundary conditions. We also study the finite size effects on the topological phase transition by comparing with 12×12 and 18×18 clusters. We find negligible changes in the transition point for these larger system sizes indicating that the location of the phase transition is already accurately captured in the $L \times L = 6 \times 6$ system size.

Using the single-particle Green's function we directly evaluate the Z_2 invariant ν,[40] where

$$(-1)^\nu = \prod_{\mathbf{k}_i \in TRIM} \tilde{\eta}_{\mu_i}, \qquad (2)$$

and $\tilde{\eta}_{\mu_i} = \langle\tilde{\mu}_i|P|\tilde{\mu}_i\rangle$ denotes the parity of the eigenstates of zero-frequency Green's functions[20] (see details in supplementary information). Fig. 2 (a)-(c) depict the dependence of the Z_2 invariant on t_{3N}/t for $U/t = 2$, 3 and 4. The open black squares denote the Z_2 invariant given by tight-binding calculations with a 200×200 system size. The open red circles indicate the Z_2 invariant calculated by QMC simulations for a 6×6 system at $U = 0$. The results are indistinguishable, confirming the accuracy of our QMC calculations in the non-interacting limit, and validating the 6×6 system size results. The location of topological phase boundary is $t_c = \frac{1}{3}t$. In the TI phase, only the M_1 point is parity odd; the other three TRIM points are parity-even (i.e. $\tilde{\eta}_\Gamma = \tilde{\eta}_{M_{2,3}} = +1$ and $\tilde{\eta}_{M_1} = -1$), so $(-1)^\nu = -1$. Across the transition upon increasing t_{3N}, $\tilde{\eta}_{M_{1,2,3}}$ change parity. Γ and M_1 are parity-even whereas $M_{2,3}$ are parity-odd, so $(-1)^\nu = 1$.

The blue solid triangles in Fig. 2 (a)-(c) depict the dependence of the Z_2 invariant on t_{3N} for $U \neq 0$. With correlations, the parity properties of the TRIM points
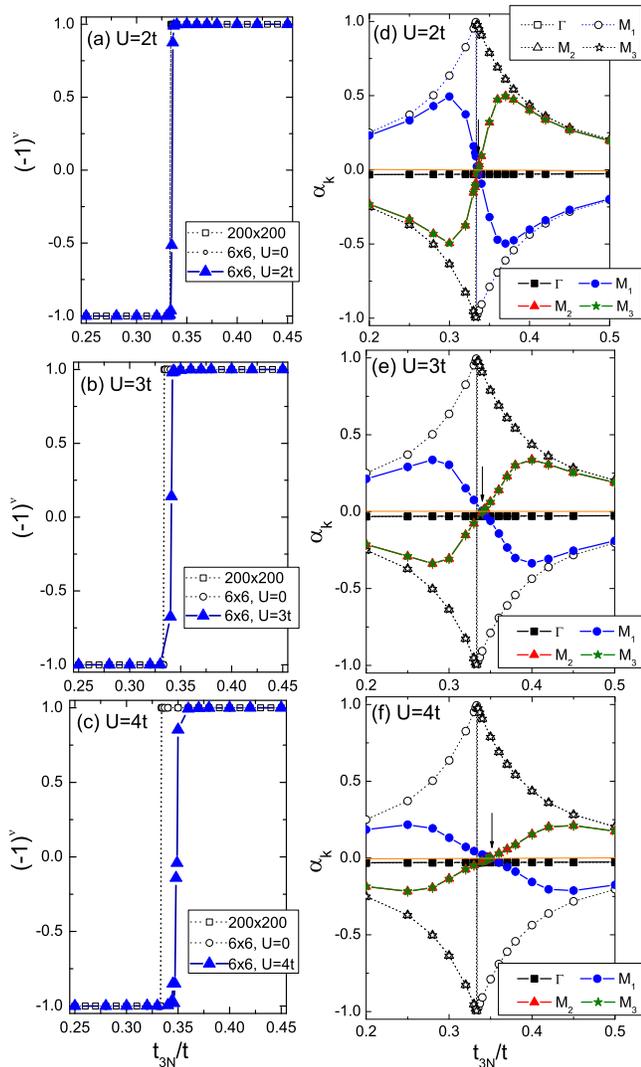
FIG. 2: (Color online) (a)-(c) Z_2 invariant at $U/t = 2$, 3 and 4 vs t_{3N}. The spin-orbital coupling is $\lambda_{SO} = 0.4t$. The black squares show the Z_2 invariant given by the tight-binding calculations with 200×200. The red circle indicates the Z_2 invariant calculated by QMC simulations with 6×6 at $U = 0$. The blue solid triangles depict the Z_2 invariant of the KMH model at $U \neq 0$. (d)-(f) show the proportional coefficient $\alpha_{\mathbf{k}}$ determined by the relation: $G_\sigma(\mathbf{k}_i, 0) = \alpha_{\mathbf{k}_i}\sigma^x$ from QMC simulations vs t_{3N}. All the open symbols indicate noninteracting cases, i.e. $U = 0$. The solid symbols denote interacting cases.

still remain and Eq. (2) to evaluate the Z_2 invariant is still valid.[20,24] Strictly speaking, at each Monte Carlo measurement, the relation $\tilde{\eta}_{\mathbf{k}} = \pm 1$ is not guaranteed. However, after a thousand QMC samplings, $\langle \tilde{\eta}_{\mathbf{k}} \rangle = \pm 1$ with tiny numerical errors. At weak interaction, the phase boundary is barely seen to deviate. At $U = 2t$, the phase boundary is numerically estimated at $t_{3N} = 0.335t$, which slightly deviates from $t_c = \frac{1}{3}t$. By increasing U, however, one can explicitly see that the interacting critical points not only deviate from $t/3$ but move towards

larger values, indicating the topological phase is stabilized by interactions. At $U = 3t$ and $4t$, the topological phase transitions take place at $t_{3N} = 0.341t$ and $0.348t$, respectively. Moreover, when $\lambda_{SO} = t$, the topological phase boundary at $U = 6t$ occurs at $t_{3N} = 0.352t$. This indicates a significant ($\sim 10\%$) shift of the topological phase boundary driven by the Hubbard interaction. Moreover, no shift as a function of U is observed in a static Hartree-Fock mean-field approximation. It is thus the quantum fluctuations originating in the interactions that are important for shifting the phase boundary and stabilizing the topological phase. We believe this is likely to be a rather general result.

Next, we investigate the single-particle Green's function in our model. The parity operator is written as $\mathbb{I} \otimes \sigma^x$,[40] and with inversion symmetry the Green's functions for each spin are simply proportional to σ^x: $G_\sigma(\mathbf{k}_i, 0) = \alpha_{\mathbf{k}_i}\sigma^x$ [or see Eq. (7) in the supplemental information]. In Fig. 2 (d)-(f) we show the proportionality coefficient $\alpha_{\mathbf{k}}$ as a function of t_{3N} for finite U. For comparison, $\alpha_{\mathbf{k}}$ in the noninteracting case is also depicted. At $U = 0$, we find the universal relations,

$$\alpha_{M_2} = \alpha_{M_3} \quad \text{and} \quad \alpha_{M_1} = -\alpha_{M_2}, \qquad (3)$$

for all values of λ_{SO} and t_{3N}. The values of α_Γ behave smoothly as t_{3N} is varied through the topological critical points. However, the α coefficients on the other TRIM points are divergent at $t_{3N} = t_c$ and change sign at a topological phase transition. At a critical point, the gap closes at the TRIM [c.f. Fig. 1 (b)] so the zero-frequency Green's functions are on the poles.[41] Irrespective of the value of λ_{SO}, the location of the sign change is always at t_c, consistent with the behavior of the Z_2 invariant.

Turning on the Hubbard interaction U, one can still observe the sign change in $\alpha_{\mathbf{k}}$ at the topological phase transition. For finite U, the Green's functions retain their σ^x-like form and the universal relations in Eq. (3) are still observed: $\alpha_{M_2} \simeq \alpha_{M_3}$ and $\alpha_{M_1} \simeq -\alpha_{M_2}$ within QMC simulation errors, independent of the value of U/t. However, the positions of $\alpha_{\mathbf{k}}$ begin to change their signs away from $t/3$, as indicated by arrows in Fig.2 (d)-(f), which label the topological phase boundaries in the interacting case. The locations for the sign change are consistent with the places where the Z_2 invariants dramatically jump. Note that at larger U the magnitude of $\alpha_{\mathbf{k}}$ gradually vanish, but a sign change is still evident.

Also in Figs. 2 (d)-(f) one can observe how the $\alpha_{\mathbf{k}}$ coefficients evolve upon increasing interactions. In the noninteracting case, the coefficients flip sign dramatically at $t_c = t/3$. However, the values of $\alpha_{\mathbf{k}}$ decrease by increasing U and the sign-flip behavior becomes more smooth with stronger interaction. This corresponds to a smeared phase boundary indicated by the Z_2 invariant changes in Figs.2 (a)-(c). Interestingly, away the topological phase transitions, e.g. $t_{3N} = 0.2t$ and $0.5t$, the coefficients $\alpha_{\mathbf{k}}$ for $U \neq 0$ seem to return to their noninteracting values. Therefore, interaction effects in $\alpha_{\mathbf{k}}$ are most apparent as t_{3N} approaches the topological phase transition points.
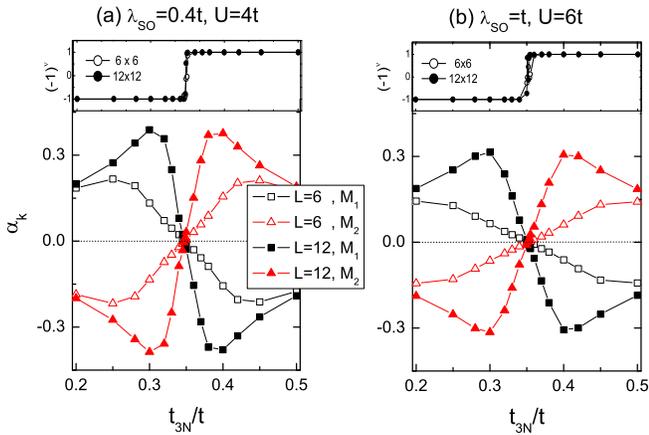
FIG. 3: (color online) The comparison of the single-particle Green's function coefficients $\alpha_{M_{1,2}}$ as a function of t_{3N} on 6×6 (open symbols) and 12×12 (solid symbols) for (a) $\lambda_{SO} = 0.4t$ and $U = 4t$ (b) $\lambda_{SO} = t$ and $U = 6t$. The insets indicate the comparison of the Z_2 invariants vs t_{3N} on the 6×6 and 12×12 clusters with the same parameters.

FIG. 4: (Color online) Single-particle excitation gap Δ_c for different values of interaction: $U/t = 0, 2, 3$ and 4 with $\lambda_{SO} = 0.4t$ on (a) 6×6 and (b) 12×12 clusters. For $U \neq 0$ the single particle gap remains open across the topological phase transition, in contrast to the behavior in a non-interacting system.

Finally, we investigate how finite size effects influence the topological phase transition boundaries with finite U. For this purpose, we compare the QMC results on 6×6 and 12×12 in Fig. 3. For a comparison for generic parameters, we consider $\alpha_{\mathbf{k}}$ at the M_1 and M_2 points for (a) $\lambda_{SO} = 0.4t$ and $U = 4t$ and (b) $\lambda_{SO} = t$ and $U = 6t$. It is evident that while stronger interaction decreases α_{M_1} and α_{M_2} in magnitude, the location of the sign change of $\alpha_{\mathbf{k}}$ barely depends on the system size. Independent of system size, α_{M_1} and α_{M_2} switch sign at the same value ot t_{3N}. Such behavior shows that the topological phase transition has a weak size dependence. The insets indicate the Z_2 invariant for the two cases, also showing a small size dependence. However, on a small size, a stronger U [e.g. the inset of Fig. 3 (b)] will lead to a less sharp boundary determined by the Z_2 invariants, compared to the $\alpha_{\mathbf{k}}$ behavior. For the same numerical accuracy, one can investigate the single-particle Green's functions on small sizes compared to the Z_2 invariant to determine the topological phase transition boundary. This result implies that the single-particle Green's function can be a powerful tool in detecting topological phase transitions in interacting systems without the need to evaluate the full topological invariant. (Although, this should certainly be checked in a few cases as it is the precise quantity that is used to distinguish the topological and non-topological phases.)

We note that the single-particle excitation gap is not a reliable quantity to detect the topological phase boundary in finite-size interacting systems. The single-particle gap should close when undertaking the topological phase transition. As shown in Fig. 4, however, the single particle gaps are finite at the phase transitions for $U \neq 0$ on the finite size simulations. Indeed, comparing the 6×6 and 12×12 systems, we can clearly see the decay ten-

dency upon increasing size. The QMC results on finite size scaling up to 18×18 confirm that around the phase boundaries the gaps vanish at $L \to \infty$. Thus the behavior of the gaps is subject to strong finite size effect and the feature of vanishing excitation can be only observed in the thermodynamic limit. Moreover, the degree to which the phase transition is obscured by the single particle gap also increases with increasing U. With 12×12, for $U = 2t$ the gap seems to close around t_c, but for $U = 4t$ the behavior prevents one from determining the topological phase boundary. Therefore, in an interacting system, one should focus on the invariant itself and the single-particle Green's function.
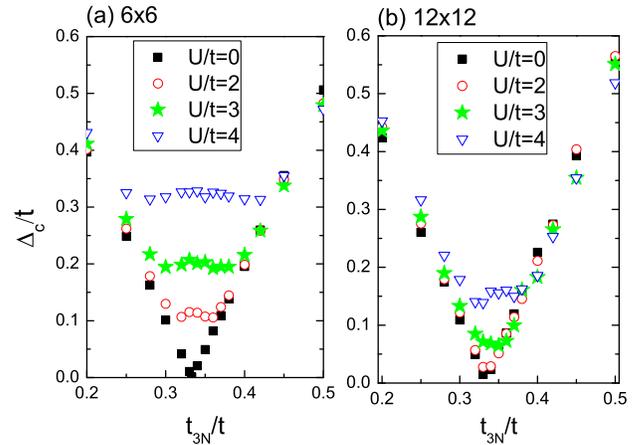
Summary.-We have studied a generalized Kane-Mele-Hubbard model with an additional third-neighbor hopping term added. In the non-interacting limit the model exhibits a topological phase transition as a function of third-neighbor hopping. By choosing moderate Hubbard interactions without inducing antiferromagnetic ordering, we study the topological phase transition in the interacting level. Using a numerically exact, fermion sign-free determinant projector QMC method, we have mapped the interaction-dependence of this phase boundary. Our main result is that interactions stabilize the topological phase by shifting the phase boundary to enlarge the topological region. This effect is absent in a static Hartree-Fock mean-field theory, which indicates it is entirely the quantum fluctuations associated with the interactions that enlarges the topological phase. We also show that the single-particle Green's function can more accurately determine the phase boundary than the Z_2 invariant (which is derived from it) for small system sizes. If this result can be reliably generalized, this could be a useful insight in large-scale "numerical searches" for real materials with topological properties. The importance

of fluctuation effects in our model also suggest that some density functional theory calculations could incorrectly predict the topological invariant of materials where quantum fluctuations are key to deciding the phase.

[1] M. Z. Hasan and C. L. Kane, Rev. Mod. Phys. **82**, 3045 (2010).
[2] J. E. Moore, Nature **464**, 194 (2010).
[3] X.-L. Qi and S.-C. Zhang, Rev. Mod. Phys. **83**, 1057 (2011).
[4] L. Fu, C. L. Kane, and E. J. Mele, Phys. Rev. Lett. **98**, 106803 (2007).
[5] J. E. Moore and L. Balents, Phys. Rev. B **75**, 121306 (2007).
[6] R. Roy, Phys. Rev. B **79**, 195322 (2009).
[7] D. Pesin and L. Balents, Nat. Phys. **6**, 376 (2010).
[8] M. Kargarian, J. Wen, and G. A. Fiete, Phys. Rev. B **83**, 165112 (2011).
[9] A. Rüegg and G. A. Fiete, Phys. Rev. Lett. **108**, 046401 (2012).
[10] B. Swingle, M. Barkeshli, J. McGreevy, and T. Senthil, Phys. Rev. B **83**, 195139 (2011).
[11] J. Maciejko, X.-L. Qi, A. Karch, and S.-C. Zhang, Phys. Rev. Lett. **105**, 246809 (2010).
[12] M. Kargarian and G. A. Fiete (2012), arXiv:1212.4162.
[13] J. Wang, A. M. DaSilva, C.-Z. Chang, K. He, J. K. Jain, N. Samarth, X.-C. Ma, Q.-K. Xue, and M. H. W. Chan, Phys. Rev. B **83**, 245438 (2011).
[14] M. Liu, C.-Z. Chang, Z. Zhang, Y. Zhang, W. Ruan, K. He, L.-l. Wang, X. Chen, J.-F. Jia, S.-C. Zhang, et al., Phys. Rev. B **83**, 165440 (2011).
[15] K. S. J. W. A. D.-J. K. G. Z. F. Steven Wolgast, Cagliyan Kurdak, arXiv:1211.5104 (2012).
[16] A. M. Turner, Y. Zhang, and A. Vishwanath, Phys. Rev. B **82**, 241102 (2010).
[17] M. Kargarian and G. A. Fiete, Phys. Rev. B **82**, 085106 (2010).
[18] Y.-M. Lu and A. Vishwanath, Phys. Rev. B **86**, 125119 (2012).
[19] X.-L. Qi, T. L. Hughes, and S.-C. Zhang, Phys. Rev. B **78**, 195424 (2008).
[20] Z. Wang and S.-C. Zhang, Phys. Rev. X **2**, 031008 (2012).
[21] Z. Wang, X.-L. Qi, and S.-C. Zhang, Phys. Rev. B **85**, 165126 (2012).
[22] L. Wang, X. Dai, and X. C. Xie, Phys. Rev. B **84**, 205116 (2011).
[23] L. Wang, H. Jiang, X. Dai, and X. C. Xie, Phys. Rev. B **85**, 235135 (2012).
[24] A. Go, W. Witczak-Krempa, G. S. Jeon, K. Park, and Y. B. Kim, Phys. Rev. Lett. **109**, 066401 (2012).
[25] C. N. Varney, K. Sun, M. Rigol, and V. Galitski, Phys. Rev. B **82**, 115125 (2010).
[26] C. N. Varney, K. Sun, M. Rigol, and V. Galitski, Phys. Rev. B **84**, 241105 (2011).
[27] M. Hohenadler, T. C. Lang, and F. F. Assaad, Phys. Rev. Lett. **106**, 100403 (2011).
[28] M. Hohenadler, Z. Y. Meng, T. C. Lang, S. Wessel, A. Muramatsu, and F. F. Assaad, Phys. Rev. B **85**, 115132 (2012).
[29] D. Zheng, G.-M. Zhang, and C. Wu, Phys. Rev. B **84**, 205121 (2011).
[30] S.-L. Yu, X. C. Xie, and J.-X. Li, Phys. Rev. Lett. **107**, 010401 (2011).
[31] J. C. Budich, R. Thomale, G. Li, M. Laubach, and S.-C. Zhang, Phys. Rev. B **86**, 201407 (2012).
[32] W. Wu, S. Rachel, W.-M. Liu, and K. Le Hur, Phys. Rev. B **85**, 205102 (2012).
[33] L. Wang, X. Dai, and X. C. Xie, Eruophys. Lett. **98**, 57001 (2012).
[34] Y. Tada, R. Peters, M. Oshikawa, A. Koga, N. Kawakami, and S. Fujimoto, Phys. Rev. B **85**, 165138 (2012).
[35] J. C. Budich, B. Trauzettel, and G. Sangiovanni (2012), arXiv:1211.3059.
[36] B. A. Bernevig, T. L. Hughes, and S.-C. Zhang, Science **314**, 1757 (2006).
[37] C. L. Kane and E. J. Mele, Phys. Rev. Lett. **95**, 146802 (2005).
[38] C. L. Kane and E. J. Mele, Phys. Rev. Lett. **95**, 226801 (2005).
[39] S. Rachel and K. Le Hur, Phys. Rev. B **82**, 075106 (2010).
[40] L. Fu and C. L. Kane, Phys. Rev. B **76**, 045302 (2007).
[41] V. Gurarie, Phys. Rev. B **83**, 085426 (2011).